Nonlinear Stress Relaxation of Molten Polymers: Experimental Verification of a New Theoretical Approach

Dino Ferri[†] and Francesco Greco*[,‡]

Polimeri Europa Research Center, Via Taliercio 14, 46100 Mantova, Italy, and Institute for Composite and Biomedical Materials (IMCB) − CNR, P. le Tecchio 80, 80125 Napoli, Italy

Received December 28, 2005; Revised Manuscript Received May 25, 2006

ABSTRACT: Measurements of damping function for step shear up to strain $\gamma = 5$ are here reported for two monodisperse well-entangled polymer melts (polystyrene and polyisoprene). At variance with the classical prediction by Doi and Edwards, which gives an universal damping function for the class entangled polymers, the two measured damping functions are different from each other, and both are less strain thinning than the universal D−E prediction. We compare then our data to a recently proposed theory [Greco, F. *Macromolecules* **2004**, *37*, 10079−10088], explicitly accounting for the equilibrium average number n_0 of Kuhn segments in a subchain. In the new theory, different n_0 values lead to different damping functions. It is shown that the independently calculated n_0 values for polystyrene ($n_0 = 25$) and for polyisoprene ($n_0 = 51$) lead to damping function predictions quite close to experiments. The number of Kuhn segments between entanglements is then a key parameter to give a consistent picture of polymer dynamics, as far as the nonlinear stress relaxation behavior is concerned.

1. Introduction

Step deformations are a critical test for the rheological properties of entangled polymer liquids.[1] It is well-known that, at sufficiently long times after a step, the stress response of these systems invariably indicates time−strain separability, i.e., factorization of the stress in a strain-dependent factor, which is the strain measure tensor, times a time-dependent relaxation function.

With the introduction of the reptation idea[2] and of the ensuing one-chain-in-a-cage theories of polymer dynamics,[3] an understanding of the phenomena following a step strain has been gained at the microscopic level, at least for monodisperse systems made up of linear chain molecules. Time−strain separability is seen to be a natural consequence of the "fast" rearrangement of a chain inside its cage, after the latter has been deformed, and of the (possibly much) slower reptative escape of the chain from the cage itself. In this scenario, Doi and Edwards[4] were able to calculate a strain measure tensor that is in good agreement with the available data, with no adjustable parameters. The case of step shear deformations merits to be explicitly cited, where the good agreement between the predicted shear damping function (the proper component of the strain measure tensor) and data extends up to fairly large strains. The shear damping function is, together with the steady-state shear viscosity, the most assessed nonlinear rheological property of entangled polymeric liquids. Its proper theoretical determination is, probably, the most impressive success of Doi−Edwards original theory.

However, some discrepancies with experiments still remain. Doi−Edwards shear damping function shows excessive strain thinning, whereby very large strain data are systematically underpredicted. Above $\gamma = 3$ (say), careful measurements give ca. 20% up to 80% higher data than predictions. In his classical 1993 review on damping functions for entangled polymers, Osaki[5] stated that "(he) personally thinks that (this difference) ... is not likely to be due to experimental error", and more recent work by other authors[6,7] also leads to this same conclusion. Thus, experimental evidence from step shear experiments points out that some modification of the original theory may be required. In fact, various attempts of modification have been proposed in the past, but based on additional hypotheses and/or parameters, which is not really satisfactory.[8]

Quite recently, one of us (F.G.) proposed a new calculation for the strain measure tensor of entangled polymeric liquids.[9] The basic physical idea that led to such proposal is quite simple. Since a subchain between entanglements is an open system made up of a rather small average number $\bar{n}$ of "particles" (Kuhn segments), fluctuations of this number are large and hence may have observable consequences. This is at variance with the standard treatment[3] of a subchain as a system in its thermodynamic limit, with negligible fluctuations. Instead, a subchain is a "small" system, which has to be dealt with through a nonstandard statistico-mechanical and thermodynamical approach. Pursuing this approach, and with no additional assumptions with respect to Doi−Edwards theory, it was demonstrated that a new strain measure tensor is obtained and that the resultant shear damping function is in (virtually) full agreement with data from literature, for both melts and solutions.[9]

Among the predictions of this new approach, of special interest is the dependence of the damping function on the equilibrium average number $\bar{n}_{eq} \equiv n_0$ of Kuhn segments in a subchain. Indeed, from the new theory, a family of damping functions should exist, with varying n_0, rather than an universal damping function, as in the Doi−Edwards approach. Testing the new theory, and the just mentioned specific prediction, are the main goals of the present paper. After an appropriate choice of two different polymeric melts, with different n_0, accurate measurements of the respective shear damping functions will be reported in the following. Since n_0 is independently determined (see below), we are in fact testing a parameter-free theory. We can anticipate here that excellent results are obtained from our experiments, which positively support the new "particle-fluctuation-inclusive" theoretical approach.

* Corresponding author: E-mail: fgreco@irc.na.cnr.it.
[†] Polimeri Europa Research Center.
[‡] Institute for Composite and Biomedical Materials.

10.1021/ma0527653 CCC: $33.50
Published on Web 07/29/2006

2. Theoretical Background

After a step deformation, when time−strain separability holds, the stress tensor **T** of an entangled polymeric liquid has the form

$$\mathbf{T} = G\mathbf{Q}(\text{strain})\, f(t) \tag{1}$$

with G an elastic modulus, $f(t)$ a relaxation function, and **Q** the strain measure tensor. Tensor **Q** is calculated from the microscopic distribution of the subchains. Let **r** be the end-to-end vector of a deformed subchain between two entanglements, and let us write $\mathbf{r} = r\mathbf{u}$, where r is the subchain span and **u** the unit vector giving its orientation in space. By calling $x = r/r_0$ the nondimensional subchain span (r_0 is the sole equilibrium length), it was shown that[9]

$$\mathbf{Q} = \frac{\sqrt{y}}{\langle x\rangle}\langle \mathbf{uu}\rangle + 3\frac{y}{\langle x\rangle}\langle x\mathbf{uu}\rangle \tag{2}$$

with y the function implicitly given by

$$y = 1 + \frac{2}{3}\left(\ln\sqrt{n_0} - \frac{\langle \ln\sqrt{n_0}x\rangle}{\langle x\rangle}\sqrt{y}\right) \tag{3}$$

and with the symbol $\langle ...\rangle$ indicating the average over the actual (x,**u**) distribution generated by the deformation. It is readily seen that the function y grows from unity to its asymptotic value $1 + (2/3)\ln\sqrt{n_0}$ with increasing the strain. The logarithmic terms in eq 3 come from the fluctuation in the Kuhn segment number of any subchain, which was mentioned in the Introduction. Hence, $y = 1$ is implied in Doi−Edwards theory. By also (artificially) suppressing the first term on the right-hand side of eq 2, Doi−Edwards original "rigorous" strain measure tensor[4] would be recovered. Notice that, with the inclusion of fluctuation effects, the strain measure tensor depends on n_0 (through the y function).

To progress from eqs 2 and 3, the assumption of "affinity" of the deformation is made, i.e., that any subchain submicroscopic end-to-end vector is deformed by the macroscopic deformation gradient tensor **E**. So, it is $r\mathbf{u} = r_0\mathbf{E}\cdot\mathbf{u}_0$, with $\mathbf{u}_0$ the original direction of the given subchain. Notice that $\mathbf{u} = \mathbf{E}\cdot\mathbf{u}_0/|\mathbf{E}\cdot\mathbf{u}_0|$ and that $x = r/r_0 = |\mathbf{E}\cdot\mathbf{u}_0|$. At undistorted equilibrium, the $\mathbf{u}_0$ unit vectors are randomly distributed. Thus, the averages in eqs 2 and 3 simply become angular integrations $\langle ...\rangle_0$ over the isotropic distribution existing prior to deformation, i.e., with $\mathbf{u}_0 = (\sin\theta\cos\varphi, \sin\theta\sin\varphi, \cos\theta)$, it is

$$\langle ...\rangle_0 = \frac{1}{4\pi}\int_0^{\pi} d\theta \sin\theta \int_0^{2\pi} d\varphi \; ... \tag{4}$$

Let us now shortly recall how n_0 is determined. The elastic modulus G in eq 1 is given by[9,10] $G = k_B T\zeta_0$, with $k_B T$ the Boltzmann constant time the temperature and ζ_0 the equilibrium number density of subchains. The entanglement molecular weigth M_e is then given by $M_e = \rho\mathscr{R}T/G$, with ρ the polymer mass density and $\mathscr{R}$ the gas constant. Hence, M_e is known from two independent measurements at equilibrium (density) and in linear viscoelasticity (modulus). The number n_0 of Kuhn segments in between two entanglements (at equilibrium) is finally calculated from the well-established relationship

$$n_0 = \frac{jM_e}{m}\frac{g^2}{C_\infty} \tag{5}$$

In eq 5, j is the number of carbon−carbon bonds per chemical monomer, m is the chemical monomer molecular weight, g is a "geometric" factor (accounting for the zigzagging spatial conformation of the polymer backbone), and C_∞ is the so-called "characteristic ratio" of the polymer, which can be independently measured or calculated.[11,12] With n_0 from eq 5, tensor **Q** is parameter-free.

In step shear, let X be the shearing direction, Y the direction normal to the shear planes, and γ the imposed strain. The shear damping function $h(\gamma)$ is simply defined as $h(\gamma) \equiv Q_{XY}(\gamma)/Q_{XY}(\gamma \to 0)$. We proceed now to compare predictions and experimental data.

Table 1. M_w and M_w/M_n by GPC and T_g by DSC of the Samples Investigated: Density at 200 °C (a) for PS and 60 °C (b) for PI; Plateau Modulus at 200 °C (a) for PS and 60 °C (b) for PI

sample	T_g (°C)	$M_w \times 10^{-3}$	M_w/M_n	ρ (g/cm^3)	G_N^0 (MPa)
PS	104	330	1.04	0.970[a]	0.208 ± 0.006[a]
PI	−61	148	1.07	0.882[b]	0.384 ± 0.007[b]

3. Experimental Section

3.1. Materials. Two nearly monodisperse linear amorphous polymers were investigated: atactic polystyrene (PS) (commercial grade produced by Polymer Laboratories) and polyisoprene (PI) (grade produced by Polimeri Europa). Both samples were prepared by anionic polymerization. The chemical microstructure of PI was determined using H NMR after dissolution in deuteriochloroform. The spectra were recorded on a Bruker AMX 300 spectrometer. The frequencies of the content of the *cis*-1,4, *trans*-1,4, and 3,4 (isopropenyl) additions were 82%, 8%, and 10%, respectively. To prevent thermal oxidation, polyisoprene was stabilized by means of two commercially available antioxidants supplied by CIBA (Irganox 565, Irgafos TNPP). No effects due to thermal degradation of the two samples were observed over the ranges of time and temperature used in this study.

Samples are characterized in Table 1. The glass transition temperatures were determined with a TA Instruments Q1000 DSC using thermograms on heating at 20 K/min, and the average molecular weight M_w and first polydispersity index M_w/M_n were determined by means of SEC operated at 25 °C with tetrahydrofuran as the mobile phase.

Concerning density data at the temperatures chosen for the step experiments, very accurate density values for polystyrene at 200 °C can be found in the literature. The value used in the present work was taken from the *Polymer Handbook*[13] and is reported in Table 1. For polyisoprene, the density was determined at 23 °C by means of a density gradient column (2-propanol−water as liquid system, ASTM method 1505). The value obtained is $\rho = 0.903$ g/cm^3. Using the volume expansion coefficient of PI ($\beta = 6.7 \times 10^{-4}$ K^{-1}),[13] the density at 60 °C was consequently calculated and is reported in Table 1.

3.2. Rheological Measurements. Equipment. Dynamic-mechanical analysis (DMA) was performed in shear with a constant strain Rheometrics mechanical spectrometer (RMS) model 800. The instrument was equipped with a force rebalance transducer able to detect torques within the range 0.02−20 N. The actuator was an air bearing motor with a strain amplitude of 0.05−500 mrad and a rotation angular frequency varying betweeen 10^{-3} and 10^2 rad/s.

The samples were compression-molded (PS at about 200 °C and PI at about 80 °C) under a pressure of 20 MPa and recovered as 25 mm diameter disks to fit the RMS tools. The linear viscoelastic functions have been measured using the parallel plate geometry (diameter 25 mm and gaps ranging between 1 and 1.2 mm). Isothermal frequency scans were performed in the range between 10^{-1} and 10^2 rad/s. The temperature was stable within 0.2 °C over the range used in this study. Strain sweeps were previously performed to ensure that the viscoelastic response was linear, and time sweeps were also performed to test the thermal stability of the samples. All tests were done under a N_2 atmosphere. The rubbery plateau modulus value was inferred for each polymer from

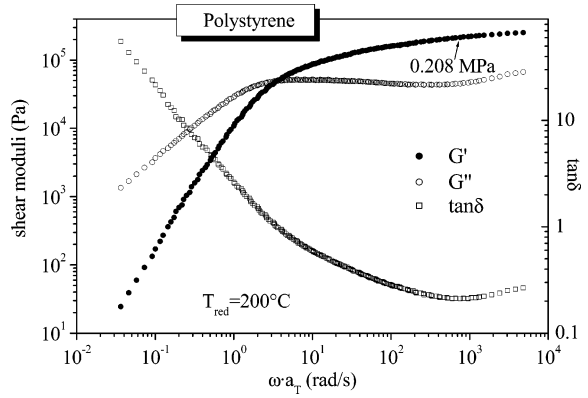

Figure 1. PS master curve reduced at 200 °C. The arrow indicates the plateau modulus as the G' value at the angular frequency where the minimum of tan δ occurs ($\omega = 762$ rad/s).

Table 2. Molecular Weight between Entanglements M_e, Geometric Factor g, Characteristic Ratio C_∞, and Number of Kuhn Segments between Entanglements n_0 for PS and PI

sample	M_e (g/mol)	g	C_∞	n_0
PS	18350 ± 600	0.83	9.6	25
PI	6350 ± 120	0.80	4.7	51

master curves reduced using both horizontal and vertical density/temperature shift factors.

Step strain experiments were performed at 200 °C for PS and at 60 °C for PI using the same rheometer equipped with the cone and plate geometry (diameter 25 mm and cone angle 0.1 rad). With this cone angle, the maximum angular displacement of the actuator (0.5 rad) in a stress relaxation test allows step strain experiments up to 5 strain units to be carried out. The nominal strain was carefully examined during the imposition of the step deformation to check the strain profile during the very short transient leading to the desired deformation. It was verified that the ideal step strain is replaced, in the real case, by a strain profile of the actuator which reaches the final strain in a finite, although very short, time interval Δt. It was found that at worst (the case with $\gamma = 5$) the transient lasts less than 0.1 s. The damping function was measured up to $\gamma = 5$ three times at each strain value investigated. For each strain value, the mean of the three measurements was taken as the best estimate for the damping function, and the standard deviation was taken as the best estimate of the error on the mean. A new sample was used for each stress relaxation test.

4. Experimental Results

4.1. Monodisperse Polystyrene ($n_0 = 25$). To calculate the plateau modulus of PS, the linear viscoelastic functions were measured at different temperatures as a function of frequency, and the master curve reported in Figure 1 was constructed. The reduction temperature is equal to that chosen during the isothermal step strain experiments (200 °C). Measurements were carried out from 160 to 230 °C every 10 °C. According to a well-established procedure,[14,15] the plateau modulus G_N^0 was taken as the G' value measured at the angular frequency value at which the minimum of tan δ was recorded ($\omega_{min} = 762$ rad/s). The value of G_N^0 is reported in Table 1 (last column) together with an error estimated by taking into account the two G' values measured at angular frequencies right above and below ω_{min}. This value is in excellent agreement with the values found in the literature for atactic polystyrene.[13,15] Using the density value for PS at 200 °C reported in Table 1, the molecular weight between entanglements M_e was calulated by means of the classical equation $M_e = \rho\mathcal{R}T/G_N^0$. The value obtained for M_e together with the estimated error is reported in Table 2. It should be noticed that the value of M_w is large enough

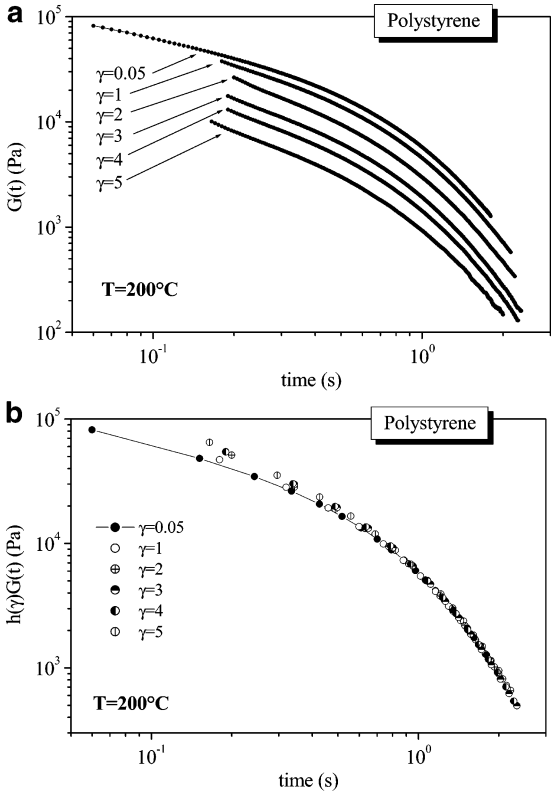

Figure 2. Linear ($\gamma = 0.05$) and nonlinear ($\gamma = 1-5$) stress relaxation modulus of PS measured at 200 °C. In (b), relaxations at large strains have been shifted onto the linear relaxation curve.

($Z \equiv M_w/M_e = 18$) to establish a fully entangled network and to ensure that segmental and terminal relaxations are well separated. Finally, using eq 5, and with $g = 0.83$ and $C_\infty = 9.6$ (see refs 12, 16, and 17), a number $n_0 = 25$ of Kuhn segments between entanglements was calculated for PS, as reported in Table 2.

In Figure 2 some of the stress relaxation modulus curves measured in step strain experiments are reported as a typical example. The sample was prepared inside the rheometer according to the usual procedure applied when the cone and plate geometry is used and let stand to equilibrate at 200 °C for 15 min. Stainless steel tools supplied by Rheometrics were used. It was verified that the curve measured when a strain value equal to 0.05 was applied lies in the linear viscoelastic regime, and this was taken as the reference curve for the vertical shift of the other stress relaxation curves (see Figure 2b). It can be seen that $G(t)$ can be factorized at "long" times, after fast relaxation processes are fully relaxed, as the product of the linear part of the response (the curve measured at $\gamma = 0.05$) times a damping function, according to the time−strain separability rule. From Figure 2b, an equilibration time for PS at 160 °C can (conservatively) be inferred as $\tau_{eq} \sim 0.3$ s.

The experimental damping function values together with the error bars are reported in Figure 3. Other data present in the literature[6] (to the authors' knowledge the most recent data set available for monodisperse PS melt) are reported for comparison. It can be noticed that the agreement between our data and those from Urakawa et al. is excellent, which is quite positive, as Urakawa et al.'s data[6] were obtained at a quite lower temperature (160 °C). From Figure 3, it is seen that the new damping function with $n_0 = 25$ convincingly better conforms to the experimental data than the D−E one. To further stress this result, the region between 3 and 5 strain units has been enlarged in Figure 4. This strain region is the most significant one in order

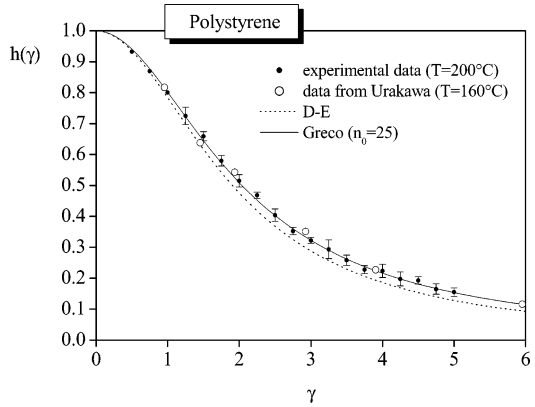

Figure 3. Damping function of PS: experimental data (black solid symbols) with the error bar, experimental data from Urakawa[6] (open symbols), universal D−E prediction (dotted line), and Greco prediction for PS ($n_0 = 25$, solid line).

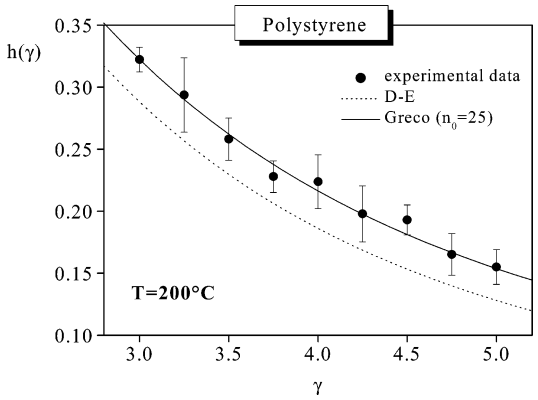

Figure 4. Damping function of PS between 3 and 5 strain units: experimental data (black solid symbols) with the error bar, universal D−E prediction (dotted line), and Greco's prediction for PS ($n_0 = 25$, solid line).

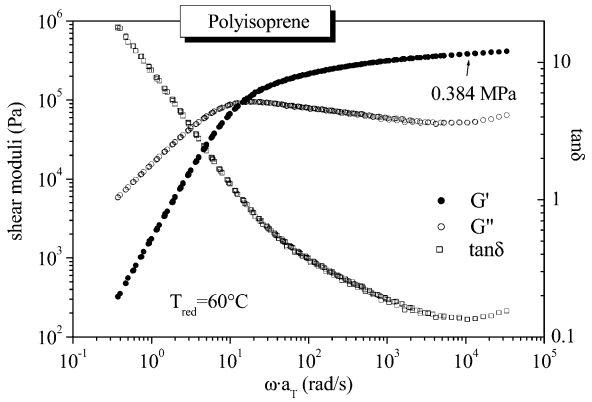

Figure 5. PI master curve reduced at 60 °C. The arrow indicates the plateau modulus identified through the angular frequency at which the minimum of the tan δ data occurs (at $\omega_{min} = 10538$ rad/s).

to highlight the differences between D−E and Greco's predictions that we are comparing in this paper. Figure 4 unambiguously proves that the new damping function is able to predict the results of nonlinear step strain experiments on PS better than the D−E universal damping function does.

4.2. Monodisperse Polyisoprene ($n_0 = 51$). To calculate the plateau modulus of PI, the linear viscoelastic functions were measured at different temperatures as a function of frequency, and the master curve reported in Figure 5 was constructed. As in the case of PS, the reduction temperature is equal to that chosen during the isothermal step strain experiments (60 °C).

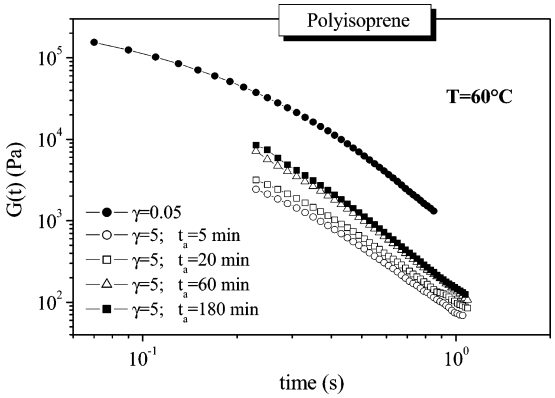

Figure 6. Linear ($\gamma = 0.05$) and nonlinear ($\gamma = 5$) stress relaxation modulus of PI measured at 60 °C after different adhesion times t_a.

Measurements were carried out from −10 to 80 °C every 10 °C. Using the same criterion previously reported for PS, with the minimum of tan δ at $\omega_{min} = 10538$ rad/s, the plateau modulus $G_N^0 = G'(\omega_{min})$ was calculated and is reported in Table 1 (last column). The value obtained lies in the range found in the literature for polyisoprene.[16−19] Using the density value for PI at 60 °C also reported in Table 1, the molecular weight between entanglements M_e was calculated. The obtained value of M_e is reported in Table 2. Also for PI, the value of M_w is high enough ($Z \equiv M_w/M_e = 23$) to establish a fully entangled network and to ensure that segmental and terminal relaxations are well separated. Using eq 5, then, with $g = 0.80$ and $C_\infty = 4.7$ as reported in Table 2 (see refs 12, 16, 17 and the Discussion and Conclusion section), a number of Kuhn segments between entanglements $n_0 = 51$ were calculated for PI.

Our first attempts to perform step strain experiments at 60 °C using the conventional procedure previously adopted for PS failed, most probably because of wall slip. Indeed, we always measured a physically meaningless too low stress relaxation modulus at large strains, a feature commonly taken as a signature of wall slip.[20] A possible way to overcome these difficulties became clear after observing that, when stuck on a metal surface at room temperature, the polyisoprene shows bad adhesion, but if left on the metal surface for a sufficient long time (typically some hours), it strongly adheres to the surface. Thus, the polymer−wall adhesion strength is time-dependent and increases with increasing adhesion time. In addition, adhesion was found to be better when disposable aluminum parallel plates were used. Very likely this happened also because the surface of these plates was not mirror polished like that of stainless steel parallel plates. Following these observations, step strain experiments on PI samples were then performed using the aluminum plates and by preparing the sample at 60 °C and leaving it in the rheometer for more than 5 h. Time sweeps were performed to check the thermal stability of the sample over this quite long time interval.

The effect of the adhesion time on the stress relaxation modulus can be appreciated in Figure 6. Here, several stress relaxation curves measured after different adhesion times imposing a strain equal to 5 are reported. The linear viscoelastic stress relaxation modulus is also reported ($\gamma = 0.05$). It can be noticed that the stress relaxation modulus curve shifts up with increasing the adhesion time. From Figure 6 it can also be noticed that the curves measured after 1 and 3 h are very similar. Further stress relaxation curves measured waiting more than 3 h were similarly undistinguishable, revealing that no more adhesion time effect was present. As a result, the measured damping function was found to be adhesion time dependent, as shown in Figure 7 for the maximum imposed strain, $\gamma = 5$. It

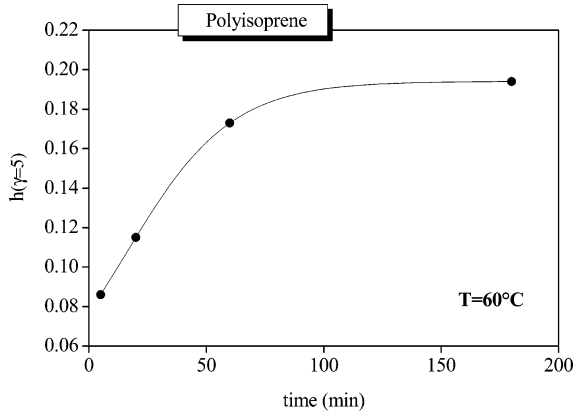

Figure 7. Adhesion time dependence of the damping function of PI measured at 60 °C and $\gamma = 5$. The $h(\gamma = 5)$ values were calculated using the stress relaxation modulus curves reported in the previous figure.

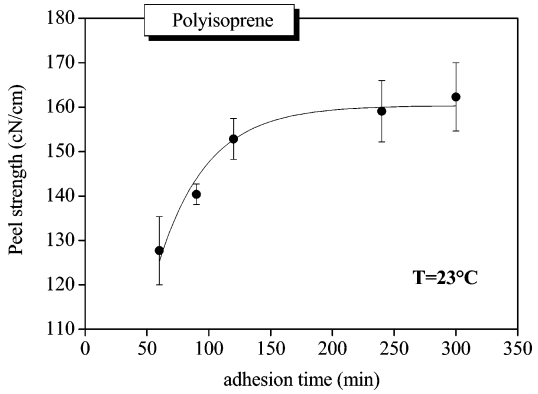

Figure 8. Adhesion time dependence of the peel strength of PI on aluminum measured at 23 °C.

can be seen that after 3 h at 60 °C the damping function has practically reached its plateau. These observations led to the choice of a waiting time of 5 h at 60 °C inside the rheometer as the time after which a complete adhesion can be obtained.

To confirm (if indirectly) that the phenomenon involved is an adhesion problem, some peel tests were performed at room temperature after different adhesion times. The time-dependent bonding of polyisoprene on aluminum measured at 23 °C is reported in Figure 8. This result is in agreement with the known fact that the peel strength develops with time by first-order kinetics.[21] It should be emphasized that the peel test discussed right above only gives indirect information on deformation and fracture mechanisms. Even if it is usually assumed that the peel strength is synonymous with the adhesive strength, a detailed analysis of peeling experiments reveals that several deformation and failure processes have to be taken into account.[22] This prevents from a quantitative correlation between the measured peel strength and the stress level developed during step strain experiments. Figure 8 is here reported just with the aim to further show that, in the step strain experiments under examination, we are facing an adhesion problem.

Another convincing evidence that a long waiting time (inside the rheometer) neatly improves the polymer−wall adhesion is given in Figure 9. Two photos are reported in this figure, showing the difference in unloading the polymer sample after a step experiments without (a) and with (b) having previously imposed an appropriate waiting time (5 h). It is apparent that, in moving apart the cone-and-plate fixtures, the polymer sample only adheres to the cone in one case (no waiting time), whereas it "sticks" on both the cone and the plate when a sufficient waiting time had been imposed before the step deformation. We think that these photos, together with the plots reported in Figures 7 and 8, indicate that the experimental difficulties encountered when a short thermal equilibration time is chosen can be overcome using the procedure adopted by the authors.

It should yet be said that, although gross wall slip phenomena were almost certainly avoided through the procedure described above, it cannot be completely excluded that some smaller level of slip occur inside the material, during the step-strain experiments. However, direct visual inspection did never reveal any kind of irregularity in the strained sample. The observed strict reproducibility of data in our experiments (see below) should also be considered: inner, randomly localized slips would most likely result in irregular variations of the measured stress in different experiments. All of these evidences, therefore, do support the reliability of our own relaxation data. (For further discussion see below, in the final section of the paper.)

In Figure 10, some stress relaxation data sets at large strains are reported, vertically shifted onto the linear relaxation curve, so as to verify the time−strain separability of PI. In fact, superposition of the relaxation curves is excellent throughout the time window examined (see Figure 10b). An equilibration time $\tau_{eq} \sim 0.2$ s can then be estimated for PI at 60 °C.

The experimental damping function values together with the error bars are finally reported in Figure 11 together with theoretical predictions. Like for PS, it can be noticed that the new damping function fits the experimental data much better than the D−E one. Again at $\gamma = 5$, for example, the datum is $h_{EXP} = 0.17$, undistinguishable from the new prediction, whereas $h_{DE} = 0.13$. The ca. 30% discrepancy with D−E theory (at this strain) has thus been completely removed.

5. Discussion and Conclusion

Let us start discussing the above-reported step experiments, now with specific emphasis on the time scales involved. Longest relaxation time τ_d of the two polymer melts investigated can be roughly estimated from their linear viscoelasticity master curves (see Figures 1 and 5), as $\tau_d \sim \omega^{-1}|_{G'(\omega)=G''(\omega)}$. This gives $\tau_d \sim 0.3$ s for PS (at 200 °C) and $\tau_d \sim 0.1$ s for PI (at 60 °C). Similar values for τ_d are obtained from the often used Menezes−Graessley formula[23] for the Rouse time τ_R

$$\tau_R \sim \frac{\eta_0 M_W}{\rho \mathcal{R} T}\left(\frac{2M_e}{M_W}\right)^{2.4} \qquad (6)$$

(with η_0 the zero-shear viscosity) plus the well-known relationship $\tau_d = 3Z\tau_R$. By means of the master curves, the zero-shear viscosity needed in eq 6 was calculated as the limiting value at low shear rates of the complex viscosity. (The lower angular frequency limit reached by the master curves was low enough to reach a clear Newtonian plateau of the viscosity.) The values obtained are $\eta_0 = 36\,500$ Pa·s for PS at 200 °C and $\eta_0 = 28\,500$ Pa·s for PI at 60 °C. With M_W, M_e, and ρ taken from Tables 1 and 2, we therefore calculate $\tau_d \sim 0.9$ s for PS and $\tau_d \sim 0.33$ s for PI, consistent with previous estimates. By looking at the time window of our relaxation experiments, then, we find that the observed time−strain separability is around the longest relaxation time τ_d, hence at times much larger than τ_R, as often reported in the literature.[5−7]

In considering step-strain experiments, Menezes and Graessley[23] and, more recently, Venerus[24] proposed some simple time scale separations criteria to be satisfied to avoid spurious results from finite strain imposition time. Specifically, by calling τ_i the strain imposition time, Menezes and Graessley require that

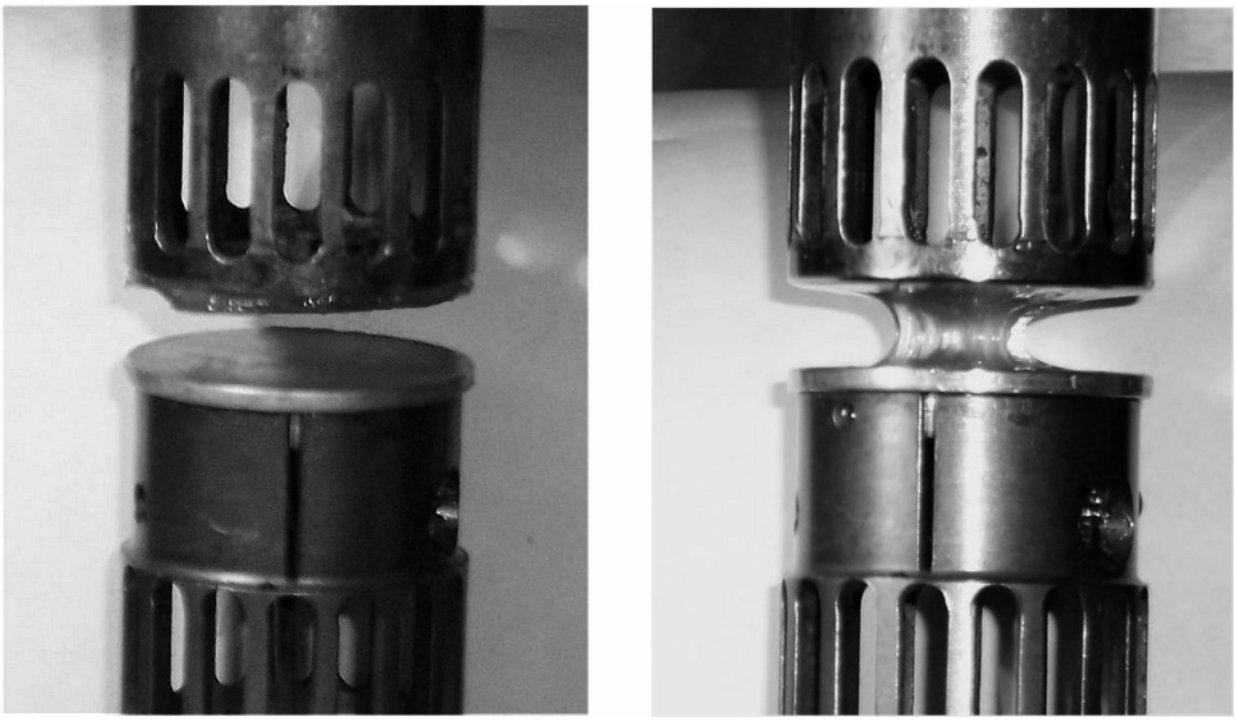

Figure 9. Photos of unloading of the PI sample after a step experiment, without (left) and with (right) having initially imposed a waiting time (5 h).

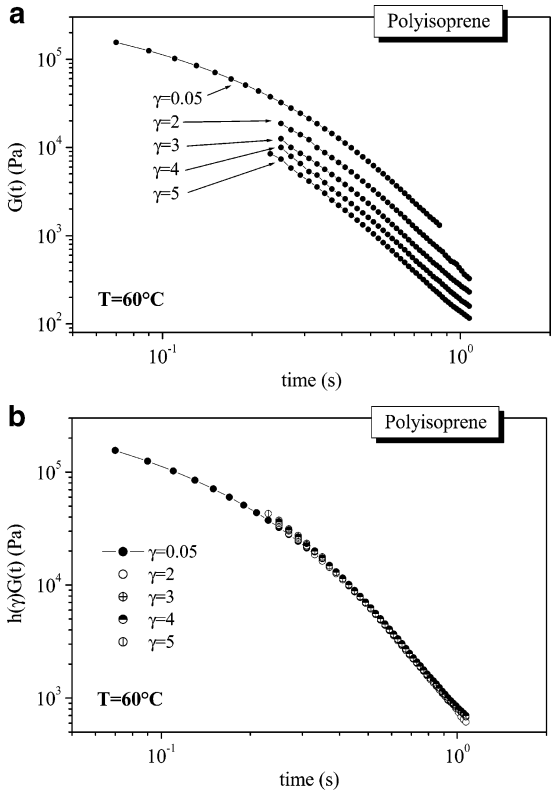

Figure 10. Linear ($\gamma = 0.05$) and nonlinear ($\gamma = 2-5$) stress relaxation moduli of PI at 60 °C. In (b), shift of the nonlinear relaxations has been imposed onto the linear viscoelastic curve.

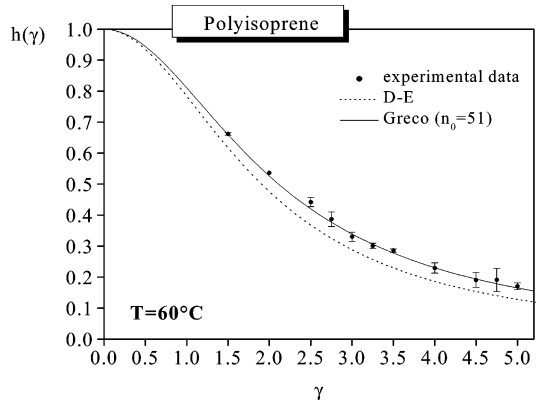

Figure 11. Damping function of PI: experimental data (black solid symbols) with the error bar, universal D−E prediction (dotted line), and Greco prediction for PI ($n_0 = 51$, solid line).

$\tau_d/\tau_i > 1$, and Venerus suggests the much stronger condition $\tau_R/\tau_i > 1$. In this respect, it has to be mentioned that our samples do not appear to fully meet these criteria. Indeed, from the estimates given above, and by considering that τ_i in our apparatus is below 0.1 s, we infer that the Menezes−Graessley criterion is matched by the two polymer melts investigated, whereas the Venerus criterion is not, and especially so for PI at 60 °C. On the other hand, Venerus himself, in his careful analysis of published data, reports that for several among the examined cases it is $\tau_R \leq \tau_i$, but anomalous relaxation was not observed, and that in fact (verbatim from[24]) "interfacial slip is the most likely explanation for anomalous step strain experiments", i.e., when anomalies are found. These conclusions might indeed apply to our own experiments. For PS at 200 °C no anomalous relaxation was ever observed, and the obtained damping function is in absolute quantitative agreement with previously published data (at 160 °C, Urakawa et al.[6]) and lies above the Doi−Edwards prediction. For PI at 60 °C slip and anomalous relaxation were found, which were afterward avoided by increasing the residence time inside the rheometer before performing the experiments. With this simple procedure, the resulting damping function is well above Doi−Edwards prediction for the PI sample, too.

To better highlight how the new damping function proves capable of describing the experimental data, the reduced chi-squared $\tilde{\chi}^2$ was calculated for the set of experimental data obtained for both monodisperse PS and PI and the three

Table 3. Reduced χ^2 Calculated Fitting the Experimental Data to the D−E Universal Damping Function and to the New Damping Function with $n_0 = 25$ (PS) and $n_0 = 51$ (PI)

sample	$\tilde{\chi}^2$ (D−E)	$\tilde{\chi}^2$ ($n_0 = 25$)	$\tilde{\chi}^2$ ($n_0 = 51$)
PS	6	0.38	1
PI	34	5.3	0.53

predictions for $h(\gamma)$ considered in this work: universal Doi−Edwards (D−E), new damping function with $n_0 = 25$ (case predicted for PS), and new damping function with $n_0 = 51$ (case predicted for PI). The reduced $\tilde{\chi}^2$ calculation was based on the following well-known equation:

$$\tilde{\chi}^2 = \frac{1}{N-p}\sum_{i=1}^{N}\frac{[y_i - h(\gamma_i)]^2}{\sigma_i^2} \tag{7}$$

in which N is the number of experimental points y_i measured together with their error bars σ_i, $h(\gamma_i)$ the corresponding predicted values, and p is the number of parameters in the theoretical damping function under scrutiny. (It is $p = 0$ for D−E universal form. For the sake of prudence, we here take $p = 1$ for the new damping function because of its n_0 dependence, but in fact n_0 is not an extra parameter.)

The $\tilde{\chi}^2$ values reported in Table 3 definitely prove that the D−E universal function is not able to capture fine details of the physics of step strain experiments of linear flexible polymer melts ($\tilde{\chi}^2 \gg 1$). On the other hand, the new damping function gives really excellent results (see the underlined entries in Table 3). Moreover, the $\tilde{\chi}^2$ values reported in Table 3 prove that the experimental data obtained for monodisperse PS better conform to the prediction for PS $n_0 = 25$ than to the prediction for $n_0 = 51$ and, vice versa, that the experimental data obtained for monodisperse PI better conform to the prediction for PI $n_0 = 51$ than to the prediction with $n_0 = 25$. In all cases, the new damping function leads to $\tilde{\chi}^2$ values lower than those from D−E theory and, correspondingly, much better describes the experimental data.

There remains to show how much the just-stated conclusion depends on the adopted n_0 values. To this aim, let us write down explicitly the formula for n_0 that we used here:

$$n_0 = \mathscr{R}T\left(\bar{l}g\,\frac{j}{m}\right)^2\frac{M_W}{R^2}\frac{\rho}{G_N^0} \tag{8}$$

(compare with eq 5). In eq 8, $\bar{l}$ is the average backbone bond length in the chemical monomer, and R^2 is the melt state (unperturbed) chain dimension, most reliably measured via small-angle neutron scattering (SANS). In the case of PS, all quantities in eq 8 are very precisely known. The monomeric term $\bar{l}g$ is taken from Flory,[25] and for the (intrinsic) chain term it is $R^2/M_W = 0.434$, as reported in ref 17, independent of temperature in the range 100−250 °C. Thus, we calculate $n_0 = 25 \pm 2$ (at most) for PS.

In the case of PI, a somewhat larger uncertainty for n_0 is expected. Indeed, the geometric factor g is different for different monomer conformations;[25] hence, an average g must be calculated, which of course depends on the microstructure of the polymer. The value of g indicated in Table 2 is obtained with cis/trans = 80%/20%, fully compatible with the chemical microstructure of our own sample, but slightly different values cannot be excluded. Similarly, the adopted value of $R^2/M_W = 0.610$, as measured in ref 12, might in fact be slightly different for our own PI sample. To stay on the safe side, then, we set a ca. ±20% possible error on our n_0 estimate as indicated in Table 2; i.e., we consider $n_0 = 51 \pm 10$. It should be immediately emphasized, however, that this is an extremely cautious estimate.

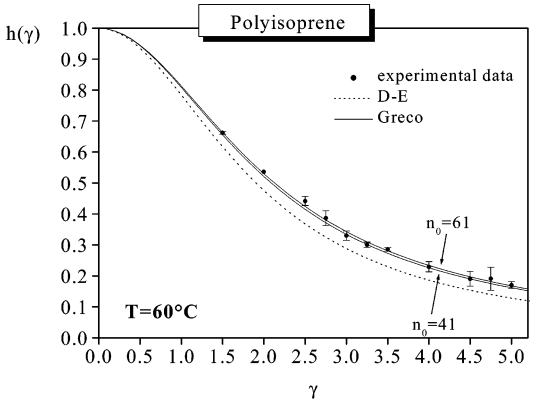

Figure 12. Damping function of PI: experimental data (black solid symbols) with the error bar, universal D−E prediction (dotted line), and Greco predictions for $n_0 = 41$ and $n_0 = 61$ (see text).

In Figure 12, our damping function data for PI are shown again, together with the predicted damping functions for $n_0 = 41$ and $n_0 = 61$, and the universal D−E curve. The calculated $\tilde{\chi}^2$ values are 1.4 (for $n_0 = 41$) and 0.48 (for $n_0 = 61$), both of them much lower than $\tilde{\chi}^2 = 34$ from D−E theory. It is clear that, in any event, the new damping function performs much better than D−E one and that the obtained improvement is a robust result.

In conclusion, we have shown in this paper that accurate measurements of damping function for polymer melts in step shear are very well described by a recently proposed theory,[9] explicitly accounting for fluctuations in the average number n_0 of Kuhn segments in a subchain. In particular, different n_0 values lead to different damping functions, at variance with the classical result by Doi and Edwards. It so appears that the number of Kuhn segments between entanglements is a key parameter to give a consistent picture of polymer dynamics as far as the nonlinear stress relaxation behavior is concerned.

Acknowledgment. Dr. Paolo Mariani is acknowledged for the peel test measurements carried out in the Polimeri Europa Research Centre of San Donato Milanese, and Dr. Fabio Bacchelli is acknowledged for its contribution to obtain the monodisperse polyisoprene. The authors also thank the anonymous referees, whose remarks and observations greatly helped in the final revision of the manuscript.

References and Notes

(1) Larson, R. G. *Constitutive Equations for Polymer Melts and Solutions*; Butterworths: Boston, 1988.
(2) de Gennes, P. G. *J. Chem. Phys.* **1971**, *55*, 572−579.
(3) Doi, M.; Edwards, S. F. *The Theory of Polymer Dynamics*; Clarendon: New York, 1986.
(4) Doi, M.; Edwards, S. F. *J. Chem. Soc., Faraday Trans. 2* **1978**, *74*, 1802−1817.
(5) Osaki, K. *Rheol. Acta* **1993**, *32*, 429−437.
(6) Urakawa, O.; Takahashi, M.; Masuda, T.; Ebrahimi, N. G. *Macromolecules* **1995**, *28*, 7196−7201.
(7) Sanchez-Reyes, J.; Archer, L. A. *Macromolecules* **2002**, *35*, 5194−5202.
(8) Among the many semiempirical corrections of the original Doi−Edwards damping function, we signal: Larson, R. G. *J. Rheol.* **1985**, *29*, 823−831, and Wagner, M. H.; Rubio, P.; Bastian, H. *J. Rheol.* **2001**, *45*, 1387−1412, both of them containing additional ad hoc parameters. This kind of work will not be discussed here. It should be mentioned that Doi and Edwards also gave, in their original papers, a "nonrigorous" strain measure tensor, which was obtained through a mathematical trick (the so-called IA approximation). Fortuitously, the IA shear damping function is in better agreement with step experiments than the "rigorous" one. However, it is well-known that the IA

approximation severely fails in other circumstances and, in the authors' opinion, no convincing possible physical motivation of the mathematical approximation used for its derivation has been advanced as yet. For these reasons, only comparison with the rigorous Doi−Edwards damping function will be considered in the present paper.

(9) Greco, F. *Macromolecules* **2004**, *37*, 10079−10088.
(10) Greco, F. *Phys. Rev. Lett.* **2002**, *88*, 108301-1-4.
(11) Mark, J. E., Ed. *Physical Properties of Polymers Handbook*; AIP: New York, 1996.
(12) Krishnamoorti, R.; Graessley, W. W.; Zirkel, A.; Richter, D.; Hadjichristidis, N.; Fetters, L. J.; Lohse, D. J. *J. Polym. Sci., Polym. Phys. Ed.* **2002**, *40*, 1768−1776.
(13) Brandrup, J., Immergut, E. H., Grulke, E. A., Eds.; *Polymer Handbook*, 4th ed.; Wiley-Interscience: New York, 1999.
(14) Wu, S. *J. Polym. Sci., Polym. Phys. Ed.* **1989**, *27*, 723−741.
(15) Lomellini, P. *Polymer* **1992**, *33*, 1255−1260.
(16) Fetters, L. J.; Lohse, D. J.; Richter, D.; Witten, T. A.; Zirkel, A. *Macromolecules* **1994**, *27*, 4639−4647.
(17) Fetters, L. J.; Lohse, D. J.; Milner, S. T.; Graessley, W. W. *Macromolecules* **1999**, *32*, 6847−6851.
(18) Gotro, J. T.; Graessley, W. W. *Macromolecules* **1984**, *17*, 2767−2775.
(19) Abdel-Goad, M.; Pyckhout-Hintzen, W.; Kahle, S.; Allgaier, J.; Richter, D.; Fetters, L. J. *Macromolecules* **2004**, *37*, 8135−8144.
(20) We signal that capillary flow curves of this sample, not reported here, revealed a spurting phenomenon at around 0.25 MPa, again a possible effect of wall slip.
(21) Wu, S. *Polymer Interface and Adhesion*; Marcel Dekker: New York, 1982.
(22) Kinloch, A. J.; Lau, C. C.; Williams, J. G. *Int. J. Fract.* **1994**, *66*, 45−70.
(23) Menezes, E. V.; Graessley, W. W. *J. Polym. Sci., Polym. Phys. Ed.* **1982**, *20*, 1817−1833.
(24) Venerus, D. C. *J. Rheol.* **2005**, *49*, 277−295.
(25) Flory, P. J. *Statistical Mechanics of Chain Molecules*; Interscience: New York, 1969.

MA0527653